PCCP

Accepted Manuscript

ROYAL SOCIETY OF CHEMISTRY

www.rsc.org/pccp

Preparation of Superhydrophobic Films based on the Diblock Copolymer P(TFEMA-*r*-Sty)-*b*-PCEMA

Ganwei Zhang,[1,2,3] Jiwen Hu,[*,2,3] Yuanyuan Tu,[2,3] Guping He,[2,3] Fei Li,[2,3] Hailiang Zou,[2,3] Shudong Lin[2,3] and Gonghua Yang[2,3]

[1]*Hubei Key Laboratory of Economic Forest Germplasm Improvement and Resources Comprehensive Utilization, Huanggang Normal University, Huanggang, P. R. China, 438000*

[2]*Guangzhou Institute of Chemistry, Chinese Academy of Sciences, Guangzhou, P. R. China, 510650;*

[3]*Key Laboratory of Cellulose and Lignocellulosics Chemistry, Chinese Academy of Sciences, P. R. China, 510650*

Abstract: The diblock copolymer poly[2,2,2-trifluoroethyl methacrylate-*r*-styrene] -*block*-poly[(2-cinnamoyloxyethyl methacrylate)] (P(TFEMA-*r*-Sty)-*b*-PCEMA) was synthesized via atom transfer radical polymerization (ATRP) methods. This copolymer underwent self-assembly in TFEMA/CH_2Cl_2 to form spherical micelles. Photocrosslinking the PCEMA domains of these micelles yielded crosslinked nanoparticles. The crosslinked nanoparticles were subsequently cast from CH_2Cl_2/methanol solvent mixtures at methanol volume fractions of more than 30% to yield rough surfaces bearing small nanobumps on micron-sized aggregations that were connected together from crosslinked nanoparticles. These surfaces were superhydrophobic, possessing a water contact angle of 161 ± 1° and a sliding angle of 6 ± 1°. Spraying these nanoparticles onto substrates exhibiting microscale roughness, such as filter paper, by a traditional coating technique also created superhydrophobic surfaces. A thin layer of nanoscaled spherical protrusions was observed on the microscaled fibers of filter paper by scanning electron microscopy (SEM) analysis. The coated filter paper samples exhibited a water contact angle and

* Corresponding author, email: hjw@gic.ac.cn, fax: 86-20-85232307

a sliding angle of 153 ± 1° and 9 ± 1°, respectively.

Keywords: Superhydrophobic, the diblock copolymer, micelles.

Introduction

Surfaces possessing water contact angles larger than 150° are considered to be superhydrophobic and superhydrophobic surfaces are very important in fundamental research and practical applications.[1] These surfaces exhibit self-cleaning behavior that is particularly important for applications such as solar panels, lenses, and mirrors that must remain clean.[2, 3] In addition, metals coated with superhydrophobic films exhibit dramatically slower corrosion rates than uncoated metals.[4] Superhydrophobic surfaces have also been shown to help reduce the accumulation of snow and ice on surfaces, and they thus have potential applications as coatings for power lines, highways and railway lines in snow or ice storms.[5-7]

In previous research, many methods have been used to fabricate superhydrophobic surfaces, such as phase separation,[8-12] block copolymer self-assembly,[13] electrospinning,[14-19] nanotube or nanofiber assembly,[18, 20-24] chemical vapor deposition,[25-27] chemical etching, plasma etching or laser treatment,[28-31] sol-gel processing,[32-34] and electrochemical anodization.[35] Most of these methods require expensive materials or severe conditions, thus limiting the applications of superhydrophobic surfaces. A more practical and less-expensive strategy might be employed to create a superhydrophobic surface using structurally stable hydrophobic nanoparticles as precursors. These particles could be dispersed into a common solvent but not dissolved, and this dispersion could then be used to fabricate a

superhydrophobic surface in a single step by adding a non-solvent. The nanoparticles could thus form aggregates exhibiting a micro-nanoscale binary structure (MNBS) via this method. These aggregates would thus provide ideal precursors for superhydrophobic surfaces, as they may exhibit roughness on both the microscale and the nanoscale, which is a key requirement for self-cleaning surfaces.[36-38] The greatest advantage of these particles is that they may be used to prepare superhydrophobic surfaces via traditional coating techniques.[38] In addition, the particles could also be sprayed onto surfaces bearing microscale roughness to yield a superhydrophobic MNBS.[39-42]

Various inorganic or organic particles, such as silica, alumina, calcium carbonate, and polymer particles, have been used to prepare hydrophobic nanoparticles.[36, 37] Silica nanoparticles are commonly used in this manner. Directly reacting silica particles with *1H,1H,2H,2H*-perfluorodecyltriethoxysilane (PFTS),[43] via surface-initiated atom transfer radical polymerization (SI-ATRP),[44] and modification with bifunctional block copolymers[37] can endow the silica particles with hydrophobicity. Meanwhile, the reaction between calcium chloride and sodium carbonate in the presence of fluoroalkyl end-capped acrylic acid allowed the preparation of fluorinated calcium carbonate particles.[45] The reduction of gold ions by poly(methylhydrosiloxane) in the presence of fluoroalkyl end-capped co-oligomeric nanoparticles yielded a novel class of fluorinated co-oligomeric nanocomposite-encapsulated gold nanoparticles.[46] Core-shell-corona particles were synthesized by a combination of emulsion polymerization and ATRP, and these

polymeric particles were subsequently fluorinated to provide low surface tension particles.[38] All of these inorganic or organic particles are stable in common solvents and provide a convenient means for the fabrication of superhydrophobic surfaces.

Recently, we reported an alternative strategy for the preparation of superhydrophobic surfaces based on diblock copolymer hollow nanoparticles from wall crosslinked vesicles or nanotubes derived from core crosslinked nonotubular micelles.[36] Hierarchical structures derived from partially fused particles could be readily tuned by either changing the solvent or the structure of the primary assembling compared to the previously mentioned strategies. Therefore, our approach may be widely applicable as a highly effective, simple and convenient strategy for the preparation of superhydrophobic surfaces.

In this report, we describe a novel class of crosslinked spherical nanoparticles that were prepared from a diblock copolymer incorporating a crosslinkable block. The diblock copolymer used in this study to prepare the crosslinked nanoparticles was P(TFEMA-*r*-Sty)-*b*-PCEMA (or (B-*r*-C)-*b*-A, Scheme 1).

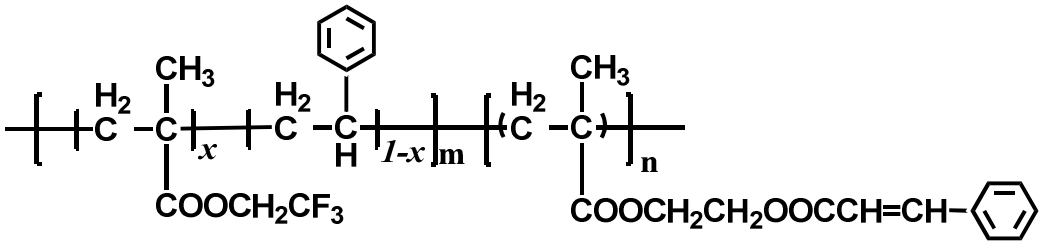

Scheme 1. Chemical structure of the diblock copolymer P(TFEMA-*r*-Sty)-*b*-PCEMA or (B-*r*-C)-*b*-A.

The PCEMA block was targeted for its demonstrated ability to undergo photocrosslinking without the need for additives.[36] PCEMA has been used previously to lock the structures of various block copolymer micelles and block-segregated solids.[47, 48] These polymers underwent self-assembly to form spherical micelles with PCEMA as the core and P(TFEMA-*r*-Sty) as the shell, which were subsequently photocrosslinked. We anticipated that the nanoparticles with crosslinked cores could be partially fused to yield hierarchical structures during the formation of the superhydrophobic surface. Moreover, we expected that the P(TFEMA-*r*-Sty) in the shell could be used as a model for not only designation of chemical composition of the formed surface but also for adjusting the surface structure owing to their different solubility in solvent, which will be reported in another paper. In addition, the precursors of spherical micelles for spherical nanoparticles were readily achieved from self-assembly than that of vesicles or nanotubes for hollow nanoparticles or nanotubes.[49] We found that a superhydrophobic surface can be readily fabricated via phase separation in one step by casting the crosslinked nanoparticle in mixed solvent, or alternatively by spraying the nanoparticle dispersion onto surfaces exhibiting microscale roughness such as filter paper by traditional coating techniques. In addition, we investigated the morphologies and wettability behavior of these superhydrophobic surfaces.

So far, there are mainly two types of approaches for the preparation of superhydrophobic surfaces that use nanoparticles derived from assembled copolymer micelles. One strategy involves the preparation of superhydrophobic surfaces based

on dip or drop-casting[50-56] or spray-coating[57, 58] of micellar solutions of block copolymers,[50, 52-56] comb copolymers,[51, 58] or random copolymers[57] in selective solvents or solvent mixtures with different selectivity. In this approach, the chemical composition and topography, which are the key factors controlling the wettability of the resulting surface, could be tuned by adjusting parameters such as the solvent properties, humidity of the air, solution concentration, copolymer structure and composition, and the dimensions and shapes of the micelles, etc. The other strategy has been mainly limited to the preparation of superhydrophobic inorganic/organic particulate coatings using building blocks such as combinations of block copolymer solutions and silica nanoparticles,[59, 60] or multilayer block copolymer micelles coated onto micrometer-sized silica particles via the layer-by-layer technique.[61] While polymeric micelles have been reported, there have been no reports on the preparation of superhydrophobic surfaces from crosslinked spherical nanoparticles composed purely of diblock copolymers.

2 Experimental Section

Materials and reagents

TFEMA was purchased from Harbin Xuefugui Chemical Co., Ltd (China), and was purified according to a previously reported procedure.[36, 62, 63] Styrene (Aladdin, 99%) was distilled over calcium hydride under reduced pressure prior to use. (Trimethylsilyloxy)ethyl methacrylate (HEMA-TMS) was synthesized and purified according to a previously reported procedure.[64] Methoxyethyl 2-bromoisobutyrate

(MEBrIB) was synthesized according to a previously reported procedure and its structure and purity were confirmed via ^{1}H NMR spectroscopy.[36, 62, 63] Copper(I) bromide (CuBr, Fluka, 98+%) was purified via stirring in acetic acid at 80 °C for over 8 h before it was subsequently washed with methanol and then dried under vacuum at room temperature. *N,N,N',N'',N'''*-Pentamethyldiethylenetriamine (PMDETA, Aldrich, 99%) was used as received. Cyclohexanone (Aladdin, 99%) was stirred overnight with calcium hydroxide before it was distilled under reduced pressure before use. Cinnamoyl chloride (Aldrich, 98%, predominantly *trans*) was used as received without further treatment. Pyridine (Aladdin, 99%) was of analytical grade and distilled over calcium hydride prior to use. Dichloromethane (CH_2Cl_2, Aladdin, 99%), tetrahydrofuran (THF, Aladdin, 99%), and hexane (Aladdin, 99%) were all of analytical grade and were distilled over sodium prior to use. The diblock copolymer P(TFEMA-*r*-Sty)-*b*-PCEMA was prepared and characterized, and the details of this synthesis are included in the Electronic Supplementary Information (ESI).

Micelle Preparation and Crosslinking

P(TFEMA-*r*-Sty)-*b*-PCEMA (40.1 mg) was fully dissolved into 1.2 mL of dry CH_2Cl_2. Subsequently, 18.8 mL of TFEMA was added dropwise to yield a bluish solution. The solution was then photolyzed in a 50 mL quartz cell for 15 h using light from a 55-W Philips-TUV lamp. The wavelength of light from the lamp was ~254 nm. The crosslinking density of the sample was determined via UV-visible spectroscopy using a Shimadzu UV-1750 instrument by comparison of the variation of the absorbance at 273 nm. The details of this technique are described in a

previous report.[65] The crosslinking density was controlled between 30% and 40% by adjusting the UV-irradiation time.

After photolysis, the solution was concentrated to 2 mL before 10 mL of hexane was added to precipitate the crosslinked product. The precipitate was rinsed thrice with 5 mL of hexane and then redispersed into 10 mL of dry CH_2Cl_2. The volume of this micellar dispersion was reduced to 5 mL by subjecting it to a flow of dry nitrogen. This procedure was repeated twice and the final micellar dispersion was prepared by dispersing the crosslinked micelles into CH_2Cl_2 at a concentration of 8 mg/mL.

Preparation of the superhydrophobic films

Particulate films were prepared by casting CH_2Cl_2/methanol dispersions (at methanol volume fractions (f_{MeOH}) ranging between 0 and 50%) of the nanoparticles onto glass slides. The dispersions were prepared by first dispersing the nanoparticles into CH_2Cl_2 at 5 mg/mL. Methanol was then added to the desired f_{MeOH}. Finally, the dilute nanoparticle dispersion used for film preparation was 2.5 mg/mL at f_{MeOH} = 50%. A particulate film was prepared by dispensing a droplet of the dispersion onto a clean glass slide and evaporating the solvent at room temperature under atmosphere with humidity of ~60%-80%.

Superhydrophobic surfaces were also prepared by spraying the crosslinked nanoparticles onto filter paper. The dispersions were prepared by dissolving the nanoparticles into CH_2Cl_2 at a concentration of 2 mg/mL. These dispersions were subsequently aero-sprayed onto filter paper using a home-built device, which was connected to a compressed nitrogen source (0.1 MPa). The distance between the

nozzle and the substrate was 20 cm.

Characterization techniques

Size exclusion chromatography (SEC) was performed at 35 °C using a Waters 1515 series system equipped with styragel HR4 and HR3 columns and a Waters 2414 refractive index (RI) detector. The system was calibrated by narrowly dispersed polystyrene standards and HPLC grade *N*,*N*-dimethylformamide (DMF) was used as the mobile phase at a flow rate of 0.60 mL/min. The SEC samples were typically prepared at concentrations of 5-10 mg/mL, and they were passed through a 0.45 μm PTFE membrane filter prior to injection. All of the ^{1}H-NMR spectra were recorded using a Bruker DMX-400 spectrometer with a Varian probe in deuterated chloroform ($CDCl_3$). Transmission electron microscopy (TEM) measurements were performed using a JEM-100CX Ⅱ microscope at an accelerating voltage of 80 kV. Micellar solutions were aero-sprayed onto nitrocellulose-covered copper grids. After they were dried at room temperature for 1 h, the samples were stained with RuO_4 vapor for 30 min prior to TEM observation. Atomic force microscopy (AFM) images of the micelles were obtained using a Bruker Multimode 8 AFM equipped with a Nanoscope Vcontroller operating in the tapping mode. The micelle solutions were directly aero-sprayed onto freshly cleaved mica surfaces. The tips used were of model RTESP of the Bruker NanoProbeTM type and had a radius of curvature typically less than 12 nm. SEM images of the superhydrophobic surfaces were obtained using a Hitachi S-4800 instrument. These SEM images were obtained after the films were coated with a thin layer of gold. Water contact angle (WCA) measurements were

performed using a contact angle measuring device (JC2000C, China) at ambient temperature with ~5 μL deionized water droplets. The advancing and receding angles were determined by probing expanding and contracting liquid droplets, respectively. For each sample, the contact angles were measured at 5-10 different positions, and the reported values corresponded to the averages of these measurements.

3 Results and Discussion

Polymer synthesis

The macroinitiator and the block copolymer were prepared via ATRP, as ATRP could be used to prepare well-defined polymers.[66] The synthesis of the macroinitiator P(TFEMA-*r*-Sty)-Br and the corresponding polymerization kinetics have been recently reported.[62] Statistical copolymers with low polydispersity indices (M_w/M_n) were prepared using MEBrIB as the initiator, and PMDETA as the catalyst system in cyclohexanone at 85 °C.

The successful synthesis of P(TFEMA-*r*-Sty)-*b*-PCEMA was confirmed via SEC and ^{1}H-NMR characterization. The polydispersity indices (M_w/M_n) obtained from SEC measurements based on PS standards were 1.14 and 1.11, respectively, for the macroinitiator and the diblock copolymer. Fig. 1 shows a ^{1}H-NMR spectrum of the diblock copolymer P(TFEMA-*r*-Sty)-*b*-PCEMA and the peak assignments. By comparing the well-defined peak integrals of δ 6.55-7.21 (m, -C_6H_5) of PS and δ 7.63 ppm (d, -CHCH-) of PCEMA, the degree of polymerization (DP), of the CEMA block

was calculated as 320. Thus, the diblock copolymer was denoted as P(TFEMA$_{41}$-*r*-Sty$_{38}$)-*b*-PCEMA$_{320}$.

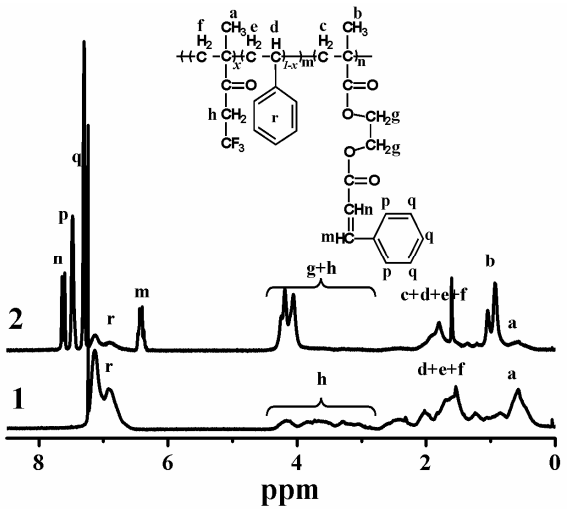

Fig. 1. ^{1}H NMR spectra of P(TFEMA-*r*-Sty) (1) and P(TFEMA-*r*-Sty)-*b*-PCEMA (2) recorded in $CDCl_3$ at 30 °C.

Table 1 lists the characteristics of the macroinitiator P(TFEMA-*r*-Sty)-Br and the diblock copolymer. While ^{1}H-NMR analysis was performed in $CDCl_3$, SEC characterization was done using DMF as the eluent and polystyrene as the calibration standards. Both the macroinitiator and the diblock copolymer were found to have low polydispersity indices. The TFEMA volume fractions f_{VB} and weight fractions f_{WB} in the macroinitiator were 51.9% and 64.2%, respectively. Meanwhile, the f_{VB} and f_{WB} values of the diblock copolymer were found to be significantly lower at 10.3% and 6.5%, respectively, because of the long chain length of the PCEMA block.

Table 1. Molecular properties of the synthesized polymers.

Polymer	M_w/M_n	M_w	x/y/b_{NMR}	$DP_{SEC,NMR}$ (a/b)	$f_{V,B}$ (%)	$f_{W,B}$ (%)	$f_{V,C}$ (%)	$f_{W,C}$ (%)
$(B_x$-*r*-$C_y)$	1.14	2.1×10^4	41/38/NA	79/---	51.9	64.2	48.1	35.8
$(B_x$-*r*-$C_y)_a$ -*b*-A_b	1.11	8.7×10^4	41/38/320	79/320	10.3	6.5	9.5	3.6

$f_{V,B}$ and $f_{V,C}$ respectively denote the volume fractions of the TFEMA or styrene units in the diblock copolymer.

$f_{W,B}$ and $f_{W,C}$ respectively denote the mass fractions of the TFEMA or styrene units in the diblock copolymer.

Micelle Preparation and Crosslinking

The diblock copolymer was initially dissolved in a good solvent CH_2Cl_2 at a certain concentration. TFEMA was then added very slowly to the solution under stirring and finally a residual milky blue micellar solution was obtained. In order to crosslink the micelles, these micellar solutions were irradiated with a UV lamp under vigorous stirring for ~15 h. The double bond conversions were determined based on the decrease in the UV absorbance at 273 nm observed after micellar photolysis in comparison with that observed prior to this treatment.

The micelles and crosslinked micelles were aero-sprayed using a home-built device and then stained with RuO_4 and OsO_4 vapor for TEM analysis. Fig. 2a and 2b show TEM images of the sprayed and stained micelles. Analogous images were obtained of the crosslinked micelles. The similar appearance of these samples suggested that our aero-spraying method can minimize the chances for the micelles to undergo morphological transitions during specimen preparation. In particular, the aero-spraying device accelerated the evaporation of the solvent TFEMA after the sample droplets had been atomized, thus minimizing opportunities for morphological transitions.[36]

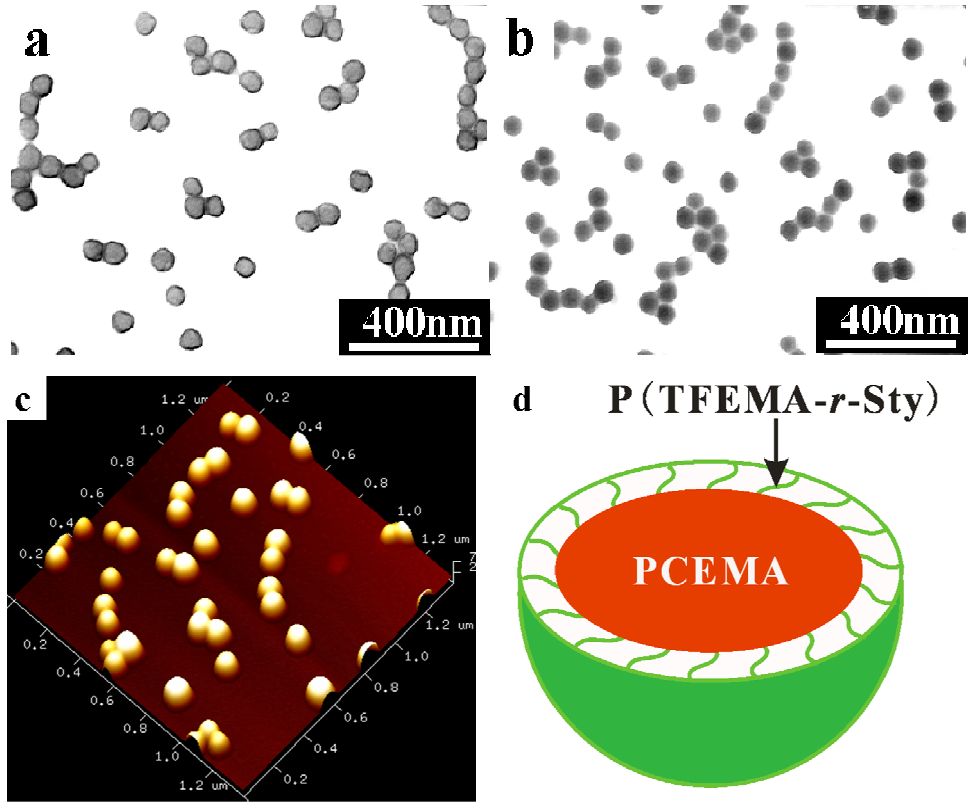

Fig. 2. TEM (a and b) and AFM (c) images of spherical micelles of the diblock copolymer. A schematic depiction of a P(TFEMA-*r*-Sty)-*b*-PCEMA micelle is also shown (d).

A TEM image of the diblock copolymer micelles that had been stained by RuO_4 is shown in Fig. 2a. The micelles were spherical nanoparticles with a thin dark rim. The diameter of the particles was approximately 70 ± 3 nm and the thickness of the rim was ~5 nm. Because TFEMA is a non-solvent for the PCEMA block, PCEMA would thus form the core of the spherical micelles (Fig. 2d). While RuO_4 can stain benzene rings, the much darker rim must have been the PS reinforced by PCEMA after solvent evaporation. The spherical structure was confirmed by the image of micelles that were stained by OsO_4, as shown in Fig. 2b. The micelles appeared as dark spherical particles with a diameter of approximately 64 ± 3 nm. Since OsO_4 can only stain the PCEMA block, the slight decrease in the diameter suggested that

the PCEMA domains formed the cores of the micelles.

The spherical morphologies of the micelles were also confirmed by AFM, as shown in Fig. 2c. The micelles exhibited a hemispherical appearance because the AFM tip could only probe the top halves of the spheres. Based on the AFM observations, the particles had an average diameter of 115 ± 5 nm and a height of 50 ± 3 nm. Since the effects of the AFM tip width and the particle flattening are very common phenomena in AFM measurements of polymer micelles, the relatively small height value in comparison with the diameter was reasonable and consistent with previous observations.[49]

Generally, rigid spheres should possess TEM diameters that are comparable with their AFM heights.[49, 67] In this case, the TEM diameter of 70 ± 3 nm was larger than the AFM height value of 50 ± 3 nm. This discrepancy suggests that the polymeric micelles had underwent a considerable degree of flattening on the silicon substrate and TEM grid. The differences between the above values also suggested that the spherical micelles were swollen.

The polymeric micelles were prepared and crosslinked in the presence of the TFEMA monomer. The crosslinking degree of PCEMA was ~40% after 24 h of photolysis under our conditions. A control experiment demonstrated that the monomer did not undergo crosslinking during UV irradiation. The TFEMA monomer was removed by CH_2Cl_2 after crosslinking treatment. The crosslinked polymeric nanoparticles could even retain their morphology in various common solvents, such as THF, chloroform, and DMF. Due to this stability, these polymer

nanoparticles have a greater potential for practical applications.

Preparation of superhydrophobic surfaces via phase separation

Particulate films of diblock polymer nanoparticles were prepared by casting CH_2Cl_2 and CH_2Cl_2/methanol dispersions of the nanoparticles at different methanol volume fractions f_{MeOH} onto a glass substrate. The water contact angle increased with the increases in the methanol volume fractions (as shown in Table 2).

Table 2. The water contact angles of spherical nanosphere-based films cast at various methanol volume fractions.

f_{MeOH}	0	15%	30%	50%
WCA (°)	105 ± 2	135 ± 2	161 ± 1	162 ± 1

When films were cast from CH_2Cl_2 dispersions of the nanoparticles, only a flat surface with some holes was obtained, as shown in Fig. 3a, 3b and 3c. The water contact angle was only 105 ± 2°. Because CH_2Cl_2 is a good solvent for the shells of the micelles, the P(TFEMA-*r*-Sty) chains were stretched and tended to form a flat particulate film, as shown in Fig. 3a, 3b and 3c. However, the evaporation of CH_2Cl_2 would help cool the surface of the liquid film and induce water condensation as well as micro-droplet formation. The holes were derived from the spaces originally occupied by the condensed water droplets, and this phenomenon has been observed previously by Widawski and coworkers.[68] Water is a non-solvent for the P(TFEMA-*r*-Sty) block, which could thus shrink. In addition, the nanoparticles could be clearly observed in the holes and thus the wall was not smooth.

Films that were partially covered by continuous flat domains, which were

interrupted by rough domains, were obtained when f_{MeOH} = 15% (Fig. 3d, 3e and 3f). The water contact angle of the particulate film prepared under these conditions was 135 ± 2°. The non-uniform surface structure exhibited by this film may be due to incomplete phase separation during the solvent evaporation process. The addition of methanol to the micellar solution did not induce phase separation, and the system had not precipitated at this point. However, methanol is a poor solvent for the diblock polymer nanoparticles and its boiling point is higher than that of CH_2Cl_2. During the solvent evaporation process, CH_2Cl_2 evaporated preferentially, and thus the residual solvent became increasingly poor for the spherical nanoparticles. As its solubility diminished, the P(TFEMA-*r*-Sty) block would shrink and condense around the PCEMA cores. In order to minimize the surface energy during the solvent evaporation process, the polymer nanoparticles needed to aggregate and phase separation occurred.[13, 69] There was not enough methanol present for perfect phase separation when f_{MeOH} = 15%, because methanol could evaporate along with CH_2Cl_2. However, when f_{MeOH} = 30%, a relatively thorough phase separation process was observed. The surface was covered by small micron-sized interconnected bumps, leading to an increase in the surface roughness, as shown in Fig. 3g, 3h and 3i. The water contact angle of the particle-based film reached 161 ± 1°. In addition, water droplets readily rolled off the surface, and a sliding angle of 6 ± 1° was observed. Xu and coworkers have obtained similar structures from micelles of polystyrene-*block*-polydimethylsiloxane (PS-*b*-PDMS).[69] When the methanol content in the copolymer solution was 50% (v/v), the system underwent precipitation.

This indicated that complete phase separation had occurred and the surface morphology was similar with that observed at f_{MeOH} = 30%. The SEM of the surface is shown in Fig. 3k, 3l and 3m. The water contact angle and sliding angle of the particle film was 162 ± 1° and 7 ± 1°, respectively.

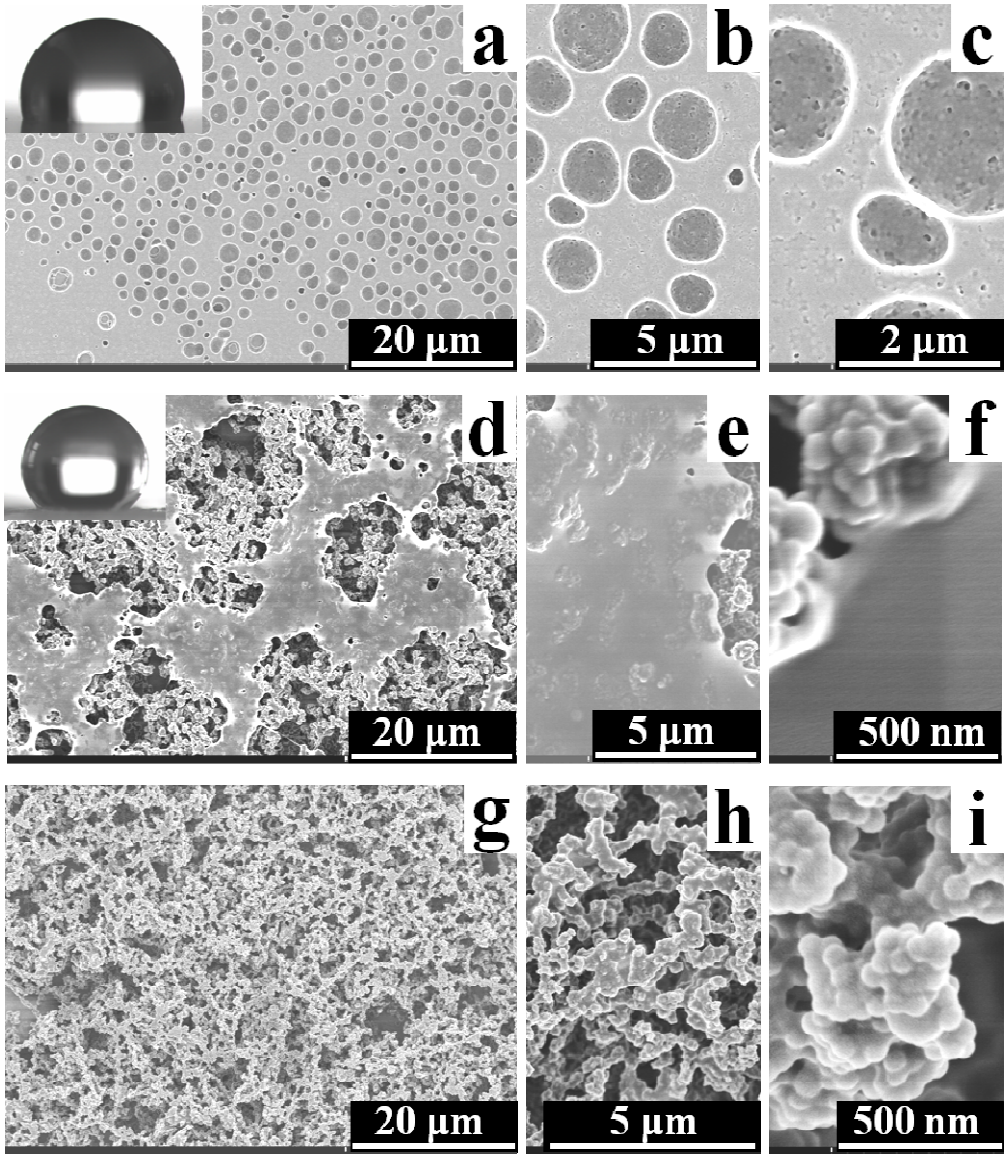

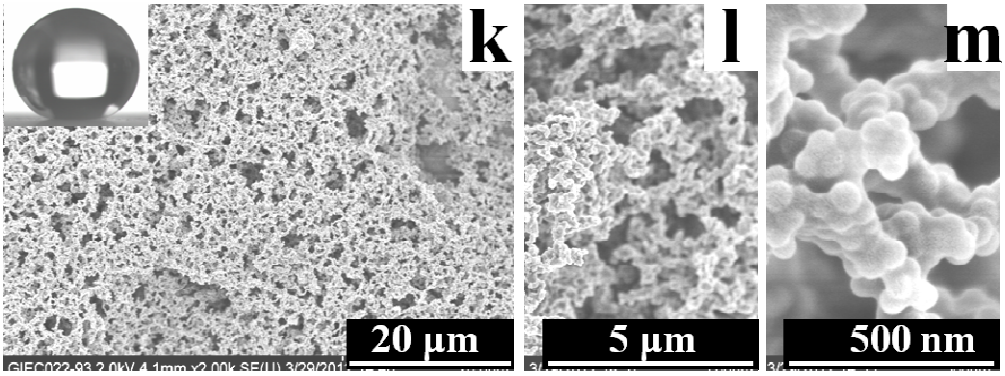

Fig. 3. SEM images of films of polymer nanoparticles cast from CH_2Cl_2/methanol at f_{MeOH} = 0% (a, b, c), 15% (d, e, and f), 30% (g, h, and i) and 50% (k, l, and m). The inset images are photographs of water droplets on the corresponding films.

Coating films on filter paper

The spherical nanoparticles can also be applied onto substrates exhibiting microscale roughness to form superhydrophobic surfaces via traditional coating methods. In order to accomplish this, the crosslinked nanoparticles were initially dispersed into CH_2Cl_2 at 2 mg/mL. These dispersions were subsequently aero-sprayed onto filter paper using a home-built device.

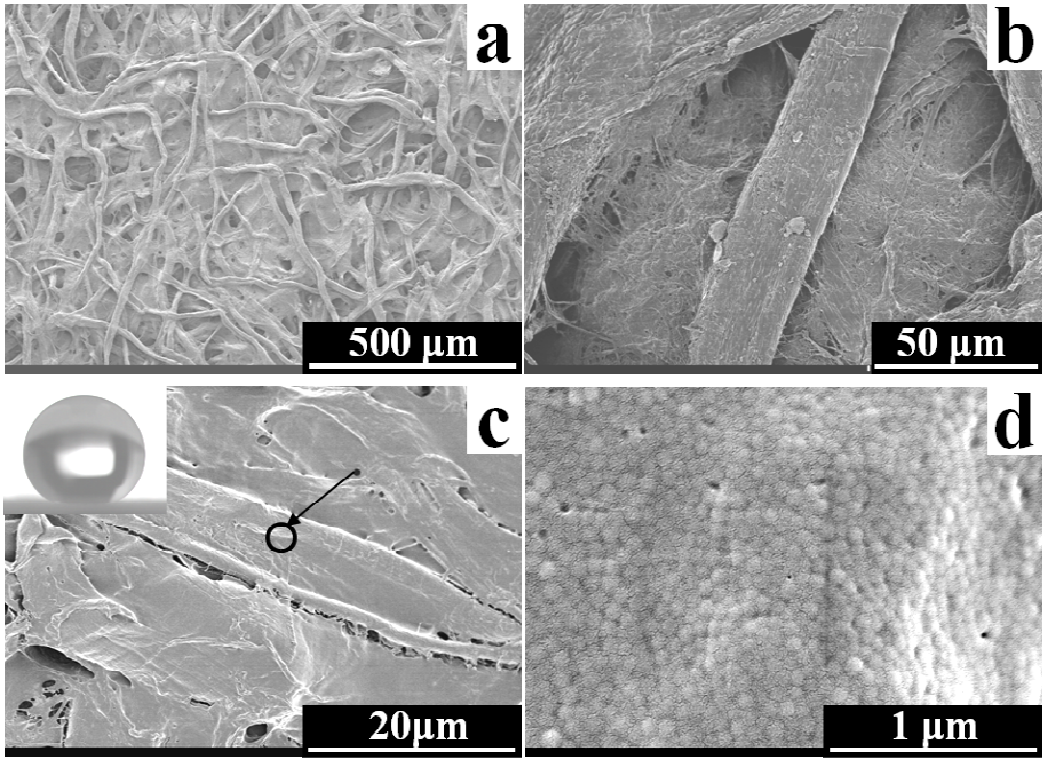

Fig. 4 SEM images of untreated filter paper (a and b) and coated filter paper (c and d, in which d is a magnified image of the area marked by the arrow in c).

The surface morphologies of untreated filter paper (Fig. 4a and 4b) and coated filter paper (Fig. 4c and 4d) samples were investigated by SEM. Fig. 4a and 4b show typical top-down views of the untreated filter paper. The untreated filter paper exhibited highly textured microscale fibers with diameters ranging between 5 and 20 µm. It was clearly evident that the filter paper was rough and did not possess a smooth surface. However, a thin layer of nanoscaled spherical protrusions was observed on surfaces of the coated filter paper samples (Fig. 4c and 4d). The combination of these hydrophobic nanoscaled protrusions and the microscaled fibers could thus form a binary structure bearing dual-scaled roughness on both the

nanoscale and the microscale, which could provide the surface with superhydrophobic properties.

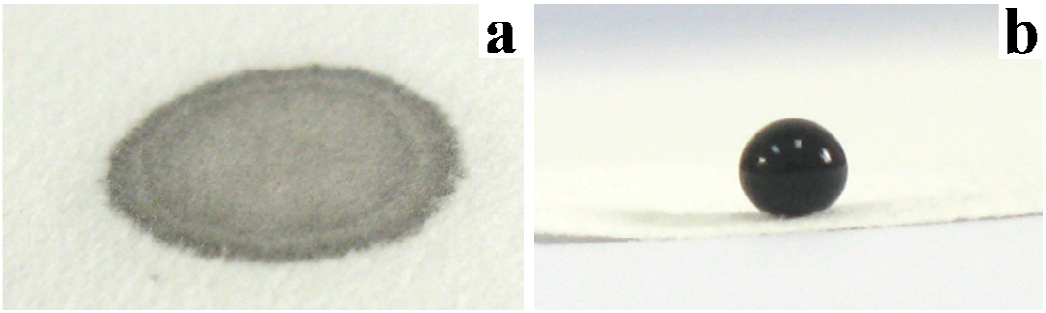

Fig. 5. Photograph of dilute black ink droplets on the surfaces of untreated filter paper (a) and coated filter paper (b).

Fig. 5a and 5b show photographs of dilute black ink droplets that were placed onto untreated filter paper and a sample of the filter paper that was coated with the nanoparticles. On the untreated filter paper, the dilute black ink droplets became absorbed by the filter paper immediately. In contrast, the dilute black ink droplet remained standing and retained an almost perfectly spherical shape on the treated filter. No noticeable sorption was observed after the droplet had been allowed to stand on the coated filter paper for 30 min. The water contact angle and the sliding angle of the coated filter paper were 153 ± 1° and 9 ± 1°, respectively.

The preparation of superhydrophobic surfaces that cover substrates bearing microscale roughness have been reported. Filter paper surfaces can be rendered superhydrophobic via "graft-on-graft" methods, during which the filter paper becomes covered with a polymer.[70] Introducing silica particles onto cotton fibers and subsequently rendering them hydrophobic with PDMS has also been applied to

readily impart cotton substrates with superhydrophobic properties.[71] These techniques might involve complicated multistage processes and the application of several treatments to attain the desired roughness and hydrophobicity. In addition, the traditional spray-coating method was also employed to impart superhydrophobicity to surfaces bearing microscale roughness using nanoparticles.[39-42] In view of the literature, all of the previous reports have been mainly concerned with the use of modified inorganic nanoparticles,[40] homopolymer nanoparticles,[39, 42] or combinations of inorganic nanoparticles and polymers[41] rather than focusing on the use of purely polymeric micelles without crosslinking to achieve a superhydrophobic surface bearing inherent microscale roughness. In our current approach, superhydrophobic surfaces with MNBS could be readily prepared by spraying diblock copolymer nanoparticles onto surfaces bearing microscale roughness, thanks to the fact that the shape of the nanoparticles could be retained during the spray-coating process compared to that of uncrosslinked micelles. The hydrophobic nanoparticles described in this research could be dispersed into common solvents such as tetrahydrofuran, chloroform or dichloromethane. Traditional coating techniques were used in this report to spray crosslinked nanoparticles onto filter paper and thus endow these surfaces with superhydrophobic properties. In addition, this strategy could be applied to impart superhydrophobic properties onto other substrates bearing micro-scale roughness. This technique provides a highly effective, simple and convenient method for the fabrication of superhydrophobic surfaces, and it is very promising.

Conclusions

In summary, we have reported a class of crosslinked nanoparticles prepared from the diblock copolymer P(TFEMA-*r*-Sty)-*b*-PCEMA. Superhydrophobic surfaces could be readily fabricated in a single step by casting mixed solvent dispersions of the crosslinked nanoparticles onto smooth substrates and relying on phase separation to provide the desired superhydrophobicity. Alternatively, traditional coating strategies could be used to apply these crosslinked nanoparticles onto substrates bearing microscale roughness, such as filter paper. A MNBS could be clearly observed via SEM. A convenient, reliable and practical method for the fabrication of superhydrophobic surfaces using polymer-based nanoparticles has been developed. This strategy is very promising and has great potential for practical use as a means to coat microtextured substrates with superhydrophobic surfaces.

Acknowledgements.

The authors thank the National Natural Science Foundation of China (No.51173204, 5120319, 21404121, and 21404122), the Guangdong Natural Science Foundation, the Special Funded Project of Pearl River in Guangzhou City of Nova of Science and Technology, Strategic Emerging Industry Development Special Fund in Guangdong Province, the Production-Education-Research Project in Guangdong Province (No. 2012B090400036), the Science and Technology Program of Guangzhou city (No. 2013J4500056), and the Science Research Special Project of Guangzhou city (No.

2014J4100216) for providing financial support.

References

1. T. Darmanin and F. Guittard, *RSC Adv.*, 2014, **4,** 50401-50405.
2. M. Nosonovsky and B. Bhushan, *Curr. Opin. Colloid Interface Sci.*, 2009, **14,** 270-280.
3. B. N. Sahoo and K. Balasubramanian, *RSC Advances*, 2015, **5,** 6743-6751.
4. Y. Y. Cheng, S. X. Lu, W. G. Xu and H. D. Wen, *RSC Adv.*, 2015, **5,** 15387-15394.
5. A. K. Kota, Y. Li, J. M. Mabry and A. Tuteja, *Adv. Mater.*, 2012, **24,** 5838-5843.
6. S. Pan, A. K. Kota, J. M. Mabry and A. Tuteja, *J. Am. Chem. Soc.*, 2013, **135,** 578-581.
7. Y. Z. Shen, H. J. Tao, S. L. Chen, L. M. Zhu, T. Wang and J. Tao, *RSC Adv.*, 2015, **5,** 1666-1672.
8. Z. J. Wei, W. L. Liu, D. Tian, C. L. Xiao and X. Q. Wang, *Appl. Surf. Sci.*, 2010, **256,** 3972-3976.
9. S. Tan, Q. Xie, X. Lu, N. Zhao, X. Zhang and J. Xu, *J. Colloid Interface Sci.*, 2008, **322,** 1-5.
10. H. Y. Erbil, A. L. Demirel, Y. Avci and O. Mert, *Science*, 2003, **299,** 1377-1380.
11. Q. D. Xie, J. Xu, L. Feng, L. Jiang, W. H. Tang, X. D. Luo and C. C. Han, *Adv. Mater.*, 2004, **16,** 302-305.
12. Z. P. Fan, W. L. Liu, Z. J. Wei, J. S. Yao, X. L. Sun, M. Li and X. Q. Wang, *Appl. Surf. Sci.*, 2011, **257,** 4296-4301.
13. Q. D. Xie, G. Q. Fan, N. Zhao, X. L. Guo, J. Xu, J. Y. Dong, L. Y. Zhang, Y. J. Zhang and C. C. Han, *Adv. Mater.*, 2004, **16,** 1830-1833.
14. L. Valtola, A. Koponen, M. Karesoja, S. Hietala, A. Laukkanen, H. Tenhu and P. Denifl, *Polymer*, 2009, **50,** 3103-3110.
15. Y. I. Yoon, H. S. Moon, W. S. Lyoo, T. S. Lee and W. H. Park, *J. Colloid Interface Sci.*, 2008, **320,** 91-95.
16. J. Zheng, A. He, J. Li, J. Xu and C. C. Han, *Polymer*, 2006, **47,** 7095-7102.
17. H. Xiang, L. Zhang, Z. Wang, X. Yu, Y. Long, X. Zhang, N. Zhao and J. Xu, *J. Colloid Interface Sci.*, 2011, **359,** 296-303.
18. J. T. McCann, M. Marquez and Y. N. Xia, *J. Am. Chem. Soc.*, 2006, **128,** 1436-1437.
19. Z. Mazrouei-Sebdani, A. Khoddami, H. Hadadzade and M. Zarrebini, *RSC Adv.*, 2015, **5,** 12830-12842.
20. A. Niemietz, K. Wandelt, W. Barthlott and K. Koch, *Prog. Org. Coat.*, 2009, **66,** 221-227.
21. A. Egatz-Gómez, J. Schneider, P. Aella, D. Yang, P. Domínguez-García, S. Lindsay, S. T. Picraux, M. A. Rubio, S. Melle, M. Marquez and A. A. García, *Appl. Surf. Sci.*, 2007, **254,** 330-334.
22. S. Zhu, Y. Li, J. Zhang, C. Lü, X. Dai, F. Jia, H. Gao and B. Yang, *J. Colloid Interface Sci.*, 2010, **344,** 541-546.
23. J. Hong and S. W. Kang, *Colloids Surf. A: Physicochem. Eng. Asp.*, 2011, **374,** 54-57.
24. D. W. Han and A. J. Steckl, *Langmuir*, 2009, **25,** 9454-9462.
25. L. B. Zhang, H. Chen, J. Q. Sun and J. C. Shen, *Chem. Mater.*, 2007, **19,** 948-953.
26. Y. Li and G. Q. Shi, *J. Phys. Chem. B*, 2005, **109,** 23787-23793.
27. X. H. Xu, Z. Z. Zhang and J. Yang, *Langmuir*, 2010, **26,** 3654-3658.
28. J. W. Krumpfer and T. J. McCarthy, *J. Am. Chem. Soc.*, 2011, **133,** 5764-5766.
29. F. Chen, D. S. Zhang, Q. Yang, X. H. Wang, B. J. Dai, X. M. Li, X. Q. Hao, Y. C. Ding, J. H. Si

and X. Hou, *Langmuir*, 2011, **27,** 359-365.
30. H. T. Yang and P. Jiang, *Langmuir*, 2010, **26,** 12598-12604.
31. J. G. Fan and Y. P. Zhao, *Langmuir*, 2010, **26,** 8245-8250.
32. L. Xu, W. Zhuang, B. Xu and Z. Cai, *Appl. Surf. Sci.*, 2011, **257,** 5491-5498.
33. N. J. Shirtcliffe, G. McHale, M. I. Newton and C. C. Perry, *Langmuir*, 2003, 19, 5626-5631.
34. Q. F. Xu, J. N. Wang and K. D. Sanderson, *ACS Nano*, 2010, **4,** 2201-2209.
35. C. A. Dai, N. Liu, Y. Z. Cao, Y. N. Chen, F. Lu and L. Feng, *Soft Matter*, 2014, **10,** 8116-8121.
36. G. P. He, J. W. Hu, G. J. Liu, Y. H. Li, G. W. Zhang, F. Liu, J. P. Sun, H. L. Zou, Y. Y. Tu and D. S. Xiao, *ACS Appl. Mater. Interfaces*, 2013, **5,** 2378-2386.
37. D. Xiong, G. J. Liu, L. Z. Hong and E. J. S. Duncan, *Chem. Mater.*, 2011, **23,** 4357-4366.
38. D. A. Xiong, G. J. Liu, J. G. Zhang and S. Duncan, *Chem. Mater.*, 2011, **23,** 2810-2820.
39. A. Milionis, L. Martiradonna, G. C. Anyfantis, P. D. Cozzoli, I. S. Bayer, D. Fragouli and A. Athanassiou, *Colloid. Polym. Sci.*, 2013, **291,** 401-407.
40. Y. Zhang, D. Ge and S. Yang, *J. Colloid Interface Sci.*, 2014, **423,** 101-107.
41. D. Ge, L. Yang, C. Wang, E. Lee, Y. Zhang and S. Yang, *Chem. Commun.*, 2015, **51,** 6149-6152.
42. A. Milionis, D. Fragouli, L. Martiradonna, G. C. Anyfantis, P. D. Cozzoli, I. S. Bayer and A. Athanassiou, *ACS Appl. Mater. Interfaces*, 2014, **6,** 1036-1043.
43. Y. C. Sheen, Y. C. Huang, C. S. Liao, H. Y. Chou and F. C. Chang, *J. Polym. Sci., Part B: Polym. Phys.*, 2008, **46,** 1984-1990.
44. H. J. Yu and Z. H. Luo, *J. Polym. Sci., Part A: Polym. Chem.*, 2010, **48,** 5570-5580.
45. H. Sawada, Y. Shikauchi, H. Kakehi, Y. Katoh and M. Miura, *Colloid. Polym. Sci.*, 2006, **285,** 499-506.
46. M. Mugisawa and H. Sawada, *Langmuir*, 2008, **24,** 9215-9218.
47. G. J. Liu, *Macromol. Symp.*, 1997, **113,** 233-248.
48. G. J. Liu, X. H. Yan, Z. Li, J. Y. Zhou and S. Duncan, *J. Am. Chem. Soc.*, 2003, **125,** 14039-14045.
49. G. Njikang, D. H. Han, J. Wang and G. J. Liu, *Macromolecules*, 2008, **41,** 9727-9735.
50. S. Desbief, B. Grignard, C. Detrembleur, R. Rioboo, A. Vaillant, D. Seveno, M. Voue, J. De Coninck, A. M. Jonas, C. Jerome, P. Damman and R. Lazzaroni, *Langmuir*, 2010, **26,** 2057-2067.
51. Z. Cui, J. Ding, L. Scoles, Q. Wang and Q. Chen, *Macromol. Chem. Phys.*, 2010, **211,** 1757-1764.
52. Z. J. Wei, W. L. Liu, C. L. Xiao, D. Tian, Z. P. Fan, X. L. Sun and X. Q. Wang, *Thin Solid Films*, 2010, **518,** 6972-6976.
53. N. Zhao, X. Zhang, X. Zhang and J. Xu, *ChemPhysChem*, 2007, **8,** 1108-1114.
54. P. H. Tung, S. W. Kuo, S. C. Chan, C. H. Hsu, C. F. Wang and F. C. Chang, *Macromol. Chem. Phys.*, 2007, **208,** 1823-1831.
55. P. H. Tung, S. W. Kuo, K. U. Jeong, S. Z. D. Cheng, C. F. Huang and F. C. Chang, *Macromol. Rapid Commun.*, 2007, **28,** 271-275.
56. Y. Wang, X. Li, H. Hu, G. Liu and M. Rabnawaz, *J. Mater. Chem. A*, 2014, **2,** 8094.
57. H. Li, Y. Zhao and X. Yuan, *Soft Matter*, 2013, **9,** 1005-1009.
58. Z. Cui, J. Ding, L. Scoles, Q. Wang and Q. Chen, *Colloid. Polym. Sci.*, 2013, **291,** 1409-1418.
59. J. T. Han, X. R. Xu and K. W. Cho, *Langmuir*, 2005, **21,** 6662-6665.
60. J. Liang, L. Wang, L. He and S. Sun, *Phys. Chem. Chem. Phys.*, 2013, **15,** 10921-10929.
61. J. Hong, W. K. Bae, H. Lee, S. Oh, K. Char, F. Caruso and J. Cho, *Adv. Mater.*, 2007, **19,** 4364-4369.
62. G. W. Zhang, J. W. Hu, G. P. He, H. L. Zou, F. Liu, C. M. Hou, H. S. Luo and Y. Y. Tu, *J. Polym.*

Sci., Part A: Polym. Chem., 2013, **51,** 1852-1864.

63. G. P. He, G. W. Zhang, J. W. Hu, J. P. Sun, S. Y. Hu, Y. H. Li, F. Liu, D. S. Xiao, H. L. Zou and G. J. Liu, *J. Fluorine Chem.*, 2011, **132,** 562-572.
64. K. L. Beers, S. G. Gaynor, K. Matyjaszewski, S. S. Sheiko and M. Moller, *Macromolecules*, 1998, **31,** 9413-9415.
65. J. Tao, G. Liu, J. Ding and M. Yang, *Macromolecules*, 1997, **30,** 4084-4089.
66. J. H. Xia and K. Matyjaszewski, *Macromolecules*, 1997, **30,** 7697-7700.
67. K. A. Ramirez-Aguilar and K. L. Rowlen, *Langmuir*, 1998, **14,** 2562-2566.
68. G. Widawski, M. Rawiso and B. Francois, *Nature*, 1994, **369,** 387-389.
69. N. Zhao, Q. D. Xie, L. H. Weng, S. Q. Wang, X. Y. Zhang and J. Xu, *Macromolecules*, 2005, **38,** 8996-8999.
70. S. H. Li, S. B. Zhang and X. H. Wang, *Langmuir*, 2008, **24,** 5585-5590.
71. H. F. Hoefnagels, D. Wu, G. de With and W. Ming, *Langmuir*, 2007, **23,** 13158-13163.